Adaptive Subspace-Based User Localization in Near-Field Regime Using Sub-Array Architecture

Larissa Rocha, Daniel Costa Araújo
Universidade de Brasília (UnB)
Email: larissa.aide1@gmail.com, daniel.araujo@unb.br

***Abstract*— Locating transmitted signals in antenna arrays has been a widely studied topic in signal processing literature. The near-field setting, particularly relevant when considering an extremely large antenna array (ELAA), poses a significant challenge as it deviates from the conventional steering vector model often used in array signal processing. In this paper, we propose an innovative method that combines adaptive subspace estimation with sub-array architecture to accurately locate users in near-field scenarios. The integration of sub-array techniques for ELAA and adaptive subspace approaches provides remarkable advantages, such as reduced computational complexity and improved performance. Our method is compared to well-established techniques in the literature, with evaluations based on root mean square error (RMSE) and cumulative distribution functions (CDFs) to characterize the statistical behavior of each method. The results demonstrate that our proposed method outperforms existing approaches in terms of precision.**

***Keywords*— Near-Field, DOA, User's Location, Sub-array, ELAA.**

I. Introduction

The development of methods to locate radiated sources through passive sensor arrays has been a major research target in the area of array signal processing. The direction of arrival (DOA) is important for obtaining direction information, which is a useful parameter for acquiring the position [1]. However, the estimation of this parameter is usually assumed to be in the far-field region, while very few works consider the near-field region [2]. The behavior of near-field electromagnetic radiation predominates close to the antenna [2], i.e., for sources located close to the array, the shape of the incident wavefront is spherical, varying nonlinearly with the position of the array. As a result, conventional DOA estimation methods, designed primarily for the far-field, become inapplicable [3].

Investigating DOA in near-field scenarios presents a multitude of possibilities, especially when considering extremely large antenna arrays (ELAA), a common feature in several key candidate technologies for sixth-generation mobile networks (6G). As the number of antennas and carrier frequency in future 6G systems increase significantly, the near-field region of ELAA will expand by orders of magnitude. Consequently, near-field communications will become crucial for future 6G mobile networks, where the distinct propagation model must be considered [4].

The importance of pinpointing near-field sources has been acknowledged, leading to the development of various approaches, including the Maximum Likelihood method [5], [6], Multiple Signal Classification (MUSIC) [7], [8] and Estimation of Signal Parameters via Rotational Invariance Techniques (ESPRIT) [8], [9]. Unfortunately, these methods come with certain limitations. For instance, most of them involve either multidimensional search or higher-order statistics (HOS) and consequently require a sufficiently large number of repetitions. In [10] and [11], the authors suggest a one-dimensional (1-D) approach based on second-order statistics with symmetric-sub-array partition to locate multiple near-field sources. This method avoids the need for computing high-order statistics, parameter pairing, or multidimensional search. The steering vectors of the appropriate sub-arrays are divided into two symmetric sub-arrays, leading to a rotational invariance property resembling a distant field in the signal subspace. However, the ESPRIT used in [10] and 2D-IFFT with fisher information (FIM) analysis in [11] for DOA estimation necessitate a large amount of data, resulting in high computational costs.

This paper introduces a groundbreaking approach to localizing user positions in the near-field region using ELAA. We employ an adaptive algorithm, PAST (Projection Approximation Subspace Tracking) [12], to monitor changes in the ELAA. This algorithm is computationally efficient, as it has a recursive update formula that eliminates the need for computationally intensive operations such as matrix inversions or eigenvalue decompositions [13]. Furthermore, it is worth noting that the precision of the estimation is influenced by not only the factors mentioned earlier but also by the number of samples utilized for the estimation process and the dimensionality of the subspace. Enhancing the number of samples while maintaining a reduced-dimensional subspace can significantly enhance the accuracy of the estimation, as exemplified in the findings of this paper, clearly illustrated through the cumulative distribution function (CDF) curve. Our approach entails two primary steps: 1) Applying the PAST algorithm to symmetric sub-arrays for DOA estimation. 2) Employing the estimated angle of arrival from each sub-array for precise range estimation through the intersection of lines method. In Section IV, we compare the performance of our PAST method compared to the 2D-IFFT [10] and ESPRIT [11] methods.

II. Signal Model

Consider a scenario in which a base station (BS) is situated near a single-antenna user equipment (UE) with an unknown position, denoted as $\mathbf{x} = [x, y]^T$, where superscript $\{\cdot\}^T$ represents the transpose. The BS is equipped with an $N+1$-element linear antenna array, with a spacing of Δ between

This work was financially supported by FAPDF, under Grant Number 00193.00001046/2021-22 , as part of the EDITAL 03/2021 - DEMANDA INDUZIDA. The authors gratefully acknowledge the funding and support provided by the agency.

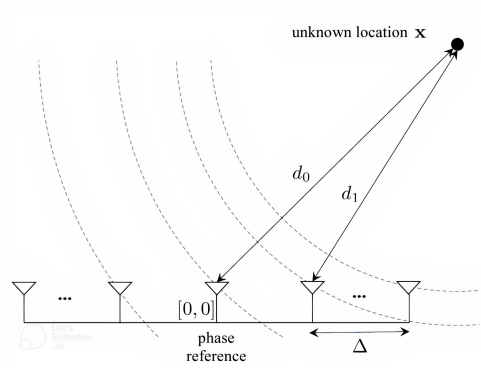

Fig. 1. In a near-field scenario with a transmitting source and a receiver array, the phase across antenna elements changes nonlinearly, while in a spatial wide-band setting, the delay across elements varies significantly [11].

each element. The array center acts as the phase reference point and the locations are represented by $\mathbf{x}_n = [n\Delta, 0]^T$, where $n \in \{-N/2, \ldots, N/2\}$, as shown in Fig. 1 [11].

The UE transmits to the BS an OFDM signal with a power of P_t and a total bandwidth of $W_b = (K+1)\Delta_f$. Here, Δ_f represents the spacing of the subcarrier and $K+1$ is the number of subcarriers. Due to a discrepancy in local oscillators, the UE has a known clock bias, denoted B.

Let $d_n = |\mathbf{x} - \mathbf{x}_n|$ represent the distance between the UE and the n-th sensor. For convenience, let $k \in \{-K/2, \ldots, K/2\}$ denote the index of the k-th subcarrier. The signal received by the n-th sensor can be expressed as follows, according to [11]:

$$Y_n[k] = \sum_{l=0}^{L} \alpha_{n,l} s[k] e^{-j\frac{2\pi}{\lambda}\epsilon_{n,l}[k]} + w_n[k], \tag{1}$$

where $s[k]$ is the pilot symbol allocated to the k-th subcarrier and term $w_n[k]$ denotes complex zero-mean Gaussian noise with a variance of $N_0/2$. The complex channel gain at antenna n with respect l-th path is characterized by $\alpha_{n,l} = \rho_{n,l} e^{j\psi_{n,l}}$, where $\rho_{n,l} = \lambda/(2\pi d_{n,l})$ and $\psi_{n,l}$ is the random phase uniformly distributed with a variance of 2π. If $l = 0$, the parameter is associated with the line-of-sight (LOS) component; otherwise, for $l > 1$, the parameters are associated with the non-line-of-sight (NLOS) components.

The parameter $\epsilon_{n,l}$ represents the phase at antenna n concerning the l-th path. Considering the array center as the phase reference point ($N = 0$) and the center subcarrier $k = 0$, the phase $\epsilon_{n,l}[k]$ at any antenna n and any subcarrier k can be expressed as:

$$\epsilon_{n,l}[k] = (d_{n,l} - d_{0,l}) + k\frac{\delta_n}{(K+1)T_s f_c}, \tag{2}$$

where $T_s = 1/W_b$. The first term, $d_n - d_0$, represents the difference in path length concerning the center antenna. The second term, $k\frac{\delta_n}{(K+1)T_s f_c}$, depends on the absolute delay δ_n and increases with the subcarrier index.

Most papers in the existing literature primarily focus on the far-field regime. In such a case, the difference in distances for linear arrays, $d_n - d_0 = \sqrt{d_0^2 + n^2\Delta^2 - 2d_0 n\Delta\cos(\theta)} - d_0$, can be approximated as $d_n - d_0 \approx -\Delta\cos\theta$ by using a Taylor expansion around $z = n\Delta/d_0 = 0$.

We assume near-field operation when the distance between the antennas is between $0.62\sqrt{(N\Delta)^3/\lambda}$ and $2(N\Delta)^2/\lambda$, where the curvature of the electromagnetic wave is significant. Additionally, we assume narrow-band operation when $N\Delta \ll c/W_b$, meaning that the signal delay between the antennas is not resolvable [6].

Under these assumptions, the phase, as described in [14], can be expressed as:

$$\epsilon_{n,l}[k] = d_{n,l} + (kr_f - 1)d_{0,l} - kr_f B, \tag{3}$$

where $r_f = \Delta f/f_c$ and B is a certain bias due to discrepancy between local oscillators. We can generalise the signal model of Eq. (1) to the matrix model:

$$\mathbf{Y} = \sum_{l=0}^{L} \mathbf{A}_l \mathbf{V}_{:,l} \mathbf{F}_{:,l}^H \mathbf{S} + \mathbf{W}, \tag{4}$$

where $\mathbf{V} \in \mathbb{C}^{N+1\times L+1}$ contains the array response to each path, so the (n,l)-th element is $\mathbf{V}_{n,l} = e^{\left(-j\frac{2\pi}{\lambda}(d_{n,l}-d_{0,l})\right)}$ and the superscript $\{\cdot\}^H$ represents Hermitian transpose. Here, $d_{n,l}$ is the distance between the n-th antenna element and the point scatterer. For $l = 0$, $d_{n,0}$ is the distance between the n-th antenna and the user. The $L+1 \times L+1$ diagonal matrix $\mathbf{A}_l = \text{diag}\,(\alpha_{0,l}, \alpha_{1,l}, \ldots, \alpha_{N,l})$. The matrix $\mathbf{F} \in \mathbb{C}^{K+1\times L+1}$, and its (k,l)-th element is $\mathbf{F}_{k,l} = e^{\left(j\frac{2\pi}{\lambda}((kr_f-1)d_{0,l} - kr_f B)\right)}$.

III. Near-Field User Position Estimation

For DOA and range estimation, we consider ELAA consisting of N_m sub-arrays, which results in the associated steering vectors of each sub-array exhibiting a far-field-like rotational invariance property in the signal subspace. By leveraging this characteristic, we can decompose the joint 2-D problem into two separate 1-D estimations. Initially, we utilize the sub-arrays to estimate their respective DOAs. We use these estimates to trace lines originating from the sub-arrays. The intersection point of these lines corresponds to the position of interest.

We partition the rows of $\mathbf{Y}$ in Eq. 4 into non-overlapping sub-arrays, each containing M elements. From the near-filed border $||\mathbf{x}|| < 2(N\Delta)^2/\lambda$, we establish an expected distance $\bar{d}$, which consists of the maximum range that we expect to find a user equipment and use near-field maximum distance to obtain

$$M \leq \sqrt{\bar{d}\lambda}/(2\Delta^2). \tag{5}$$

The sub-array m corresponds to the observations at antennas $(m-1)M+1$ through mM, with array center $\tilde{x}_m = x_{N/2} + [\Delta((m)M + 1 + M/2, 0]^T$. In this case, the indexing for m starts at 1. The total number of sub-array is $N_m = \lfloor\frac{N+1}{M}\rfloor$, assuming N is divider by M.

Each sub-array collects its signal from its respective antenna sub-array to process them and extract the subspace. The received signal at the mth sub-array is defined as $\mathbf{Y}_m \in \mathbb{C}^{M\times K+1}$. For subspace estimation, we first remove the pilot contribution by performing the following operation:

$$\hat{\mathbf{Y}}_m = \mathbf{Y}_m \mathbf{S}^H (\mathbf{S}\mathbf{S}^H)^{-1}. \tag{6}$$

Once the pilot is removed, the signal is processed by the adaptive algorithm of subspace estimation. After that, we can use the rotational invariance of the subspace to extract the angle. The method is detailed in the subsequent subsection.

A. DOA Estimation

Leveraging the rotational invariance inherent to each sub-array, we employ the PAST algorithm to estimate their respective subspaces. Once convergence is reached, this algorithm is consistently extended to successive sub-arrays, utilizing computations grounded in the final subspace estimate derived from the preceding sub-array (designated as $m-1$).

The PAST estimation consists of an interpretation of the signal subspace as the solution of a projection-like unconstrained minimization problem, which is solved using recursive least-squares approaches by appropriately approximating the projection. The dominant subspace estimation consists in minimizing the approximated scalar cost function [12], [13]:

$$J(\mathbf{U}_m) = \mathbf{E}\left\{\left\|\hat{\mathbf{Y}}_m - \mathbf{U}_m\mathbf{U}_m^H\hat{\mathbf{Y}}_m\right\|^2\right\}. \tag{7}$$

Suppose that $\mathbf{U}_m = \hat{\mathbf{U}}_m\mathbf{Q}$ represents a subset of eigenvectors for the covariance matrix $\mathbf{C} = \mathbf{E}\{\hat{\mathbf{Y}}_m\hat{\mathbf{Y}}_m^H\}$, with $\hat{\mathbf{U}}_m \in \mathbb{C}^{M\times r}(r < M)$ and r being the rank. The matrix $\mathbf{Q} \in \mathbb{C}^{r\times r}$ can be considered an arbitrary unitary matrix. When the cost function $J(\mathbf{U}_m)$ reaches its lowest possible value, $\hat{\mathbf{U}}_m$ will not consist of any eigenvectors, but rather the r most significant ones [12].

To minimize the cost function $J(\mathbf{U}_m)$, we employ the well-established RLS algorithm. This can be achieved by reformulating the cost function as follows:

$$J'(\mathbf{U}_m(k)) = \sum_{i=1}^{k}\beta^{k-i}\left|\hat{\mathbf{Y}}_m(i) - \mathbf{U}_m(k)\mathbf{U}_m^H(k)\hat{\mathbf{Y}}_m(i)\right|^2. \tag{8}$$

In this case, an exponentially weighted sum with the forgetting factor β replaces the expectation operator. When the forgetting factor is set to 1, all samples receive equal weight, ensuring that the previous data are not forgotten. By adjusting the forgetting factor to a value between 0 and 1 ($0 < \beta < 1$), the resulting algorithm can be used to track nonstationary changes in the sources, as outlined in [13].

We can modify the cost function in Eq. (8) by approximating $\mathbf{U}^H\hat{\mathbf{Y}}m(i)$ as $\mathbf{U}^H(i-1)\hat{\mathbf{Y}}m(i)$. This approximation results in an alternative cost function:

$$J''(\mathbf{U}(k)) = \sum_{i=1}^{k}\beta^{k-i}\left\|\hat{\mathbf{Y}}_m(i) - \mathbf{U}_m(k)\mathbf{U}_m^H(i-1)\hat{\mathbf{Y}}_m(i)\right\|^2. \tag{9}$$

By defining $\hat{\mathbf{Y}}'_m(i) = \mathbf{U}_m^H(i-1)\hat{\mathbf{Y}}_m(i)$, we can further simplify the expression as follows:

$$J''(\mathbf{U}_m(k)) = \sum_{i=1}^{k}\beta^{k-i}\left\|\hat{\mathbf{Y}}_m(i) - \mathbf{U}_m(k)\hat{\mathbf{Y}}'_m(i)\right\|^2. \tag{10}$$

Similar to the cost function of the RLS method, this cost function is quadratic. The only distinction is that an error vector $\mathrm{e}(k)$ is required in this instance rather than an error scalar $\mathrm{e}(k)$. We conclude that we may approximately minimize the original cost function $J(\mathbf{U}_m)$ by using RLS with the input signal $\hat{\mathbf{Y}}'_m(k) = \mathbf{U}_m^H(k-1)\hat{\mathbf{Y}}_m(k)$ and the desired signal $\hat{\mathbf{Y}}_m$. Consequently, the PAST algorithm may be summarized in the Algorithm 1 [13]. The variables $\mathbf{h}(k)$ and $\mathbf{g}(k)$ are utilized in the equations to calculate the RLS in between steps.

Algorithm 1 The PAST algorithm for tracking the signal subspace

If $m = 1$: Initialize $\mathbf{P}(0)$ and $\mathbf{U}(0)$ randomly and appropriately. If $m > 1$: Initialize using the estimates from the $(m-1)$-th sub-array.

for $k = 1, 2, \ldots$ **do**
$\hat{\mathbf{Y}}'_m(k) = \mathbf{U}^H(k-1)\hat{\mathbf{Y}}_m(k)$
$\mathbf{h}(k) = \mathbf{P}(k-1)\hat{\mathbf{Y}}'_m(k)$
$\mathbf{g}(k) = \mathbf{h}(k)/\left[\beta + \left(\hat{\mathbf{Y}}'_m(k)\right)^H\mathbf{h}(k)\right]$
$\mathbf{P}(k) = \beta^{-1}\mathrm{tri}\left\{\mathbf{P}(k-1) - \mathbf{g}(k)\mathbf{h}^H(k)\right\}$
$\mathrm{e}(k) = \hat{\mathbf{Y}}_m - \mathbf{U}(k-1)\hat{\mathbf{Y}}'_m(k)$
$\mathbf{U}_m(k) = \mathbf{U}_m(k-1) + \mathrm{e}(k)\mathbf{g}^H(k)$
end for

To ensure that the matrix $\mathbf{P}(k) \approx \mathbf{C}^{-1}(k)$ is symmetric, we use the notation $\mathrm{tri}\cdot$ to indicate that only the upper triangular portion of the argument is calculated,and its transpose is replicated to the lower triangular part. As a result, the algorithm avoids the need for any matrix inversions, with the most complex operation being scalar division [12]. The interested reader can find the proofs in [15].

It is essential to understand that the converged $\mathbf{U}_m$ does not directly contain the eigenvectors of the correlation matrix. The reason behind this is that the cost function, once minimized, does not lead to a unique solution. In other words, there could be multiple $\mathbf{U}_m$ matrices that minimize the cost function, and they might not necessarily correspond to the eigenvectors of the correlation matrix. Nonetheless, the product $\mathbf{U}_m\mathbf{U}_m^H$ is unique, and it represents the signal subspace projection matrix.

The columns of $\mathbf{U}_m$ that minimize $J(\mathbf{U}_m)$ constitute an orthonormal basis for the signal subspace generated by the dominant eigenvectors r of the correlation matrix. Consequently, it is feasible to determine the angle from the most representative column, which corresponds to the first column of the $\mathbf{U}_m$ matrix. This can be done by rewriting it in the form of two vectors: $\mathbf{u}_1 = [e^{-j\omega_0}, \ldots, e^{-j\omega(M-2)}]$ and $\mathbf{u}_2 = [e^{-j\omega_1}, \ldots, e^{-j\omega(M-1)}]$. Given the steering vector for a linear array, $\omega_i = 2\pi\frac{d}{\lambda}i\cos\theta$, it follows that $\omega_i - \omega_{i-1} = 2\pi\frac{d}{\lambda}\cos\theta$. Therefore, we can estimate the θ_m of a sub-array as:

$$\hat{\theta}_m = \cos^{-1}\left(\frac{\lambda}{2\pi Md}\sum_{i=1}^{M-1}\arg\left(\mathrm{diag}[\mathbf{u}_1^*]\mathbf{u}_2\right)_i\right), \tag{11}$$

where $\arg\left(\mathrm{diag}[\mathbf{u}_1^*]\mathbf{u}_2\right)$ yields a vector containing the arguments of the complex number entries of the vector $\mathrm{diag}[\mathbf{u}_1^*]\mathbf{u}_2$.

B. Range estimation

Two critical parameters are required to determine the location of a UE: the angle of arrival of the signal and the distance between the user and the antenna. Having presented a method for estimating the angle, we utilize this parameter to mathematically express a line originating from two sub-arrays. We then calculate the intersection point of the sub-array lines, following a similar approach as presented in [11] and [10].

Line intersections occur when two or more lines converge at a shared point. In this context, we consider the lines as the distances we aim to determine, and the common point represents the UE with coordinates $\mathbf{x} = [x, y]^T$ [16]. Considering the relatively stable angles and distance values across sub-arrays, our emphasis is on the angle and distance of both the initial and final sub-arrays. This enables us to succinctly represent the coordinates as follows:

$$x = \frac{\tilde{x}_A \cdot \tan(\hat{\theta}_A) - \tilde{x}_B \cdot \tan(\hat{\theta}_B)}{\tan(\hat{\theta}_A) - \tan(\hat{\theta}_B)} \tag{12}$$

$$y = x \cdot \tan(\hat{\theta}_A) - d_A \cdot \tan(\hat{\theta}_B), \tag{13}$$

where, $\tilde{x}_A$ represents the center of first sub-array, $\tilde{x}_B$ denotes the center of last sub-array, $\hat{\theta}_A$ refers to the angle estimated by PAST for first sub-array, and $\hat{\theta}_B$ corresponds to the angle estimated by PAST for last sub-array. Incorporating both the angle and range estimation methods, we summarize the proposed user location Algorithm 2 for sub-array localization.

Algorithm 2 Sub-array Localization

Assume the number of antennas per sub-array as in Eq. 5.
Select two sub-arrays to trace the lines. Choose the first and the last ones.
for $m = \{1, M\}$ **do**
  Collect $\mathbf{Y}_m$.
  Verify the most recent estimate of $\mathbf{U}_m$.
  Obtain $\mathbf{U}_m$ using the PAST Algorithm 1. If no previous estimate of $\mathbf{U}_m$ exists for other sub-arrays, initialize as a zero matrix.
  Estimate $\hat{\theta}_m$ using Eq. 11.
  Calculate the center of the sub-array: $\tilde{x}_m = x_{N/2} + [\Delta((m)M + 1 + M/2, 0]^T$.
end for
Calculate x and y using Eq. (12) and Eq. (13).
Determine the UE position as $\mathbf{x} = [x, y]^T$.

It is essential to highlight that the range estimation, which relies on the curvature of the electromagnetic wave, is not influenced by the bias B. This stands in contrast to the use of pilots spread across the frequency domain for delay estimation. Furthermore, it is possible to combine both techniques to estimate the bias B more effectively.

IV. Numerical Results

We consider a scenario at a carrier f_c of 28 GHz ($\lambda \approx 1.07$ cm), a bandwidth W of 100 MHz, $c = 0.3$ m/ns $N_0 = 4.0049 \times 10^{-9}$ mW/GHz, a transmit power P_t of 1 mW (with $E\{|s[k]|\}^2 = P_t/W$) and $K+1 = 257$ subcarriers with QPSK pilots. The UE has bias $B = 20$ m. The array has $N+1 = 129$ elements spaced at $\lambda/2$, corresponding to a total size of 69.11 cm and a far-field distance of 89 m. To test the performance of the algorithm, 500 Monte Carlo simulations are performed.

To validate the effectiveness of the method proposed in this paper (PAST), including an enhanced variant (PAST with SVD-based initialization of the first sub-array), we conduct a comparative analysis. We contrast the RMSE and CDF curves with established techniques from the literature, 2D-IFFT [10] and SPRIT [11]. All estimators employ the sub-array approach and are tested in a multipath propagation setting that includes both LOS and NLOS components. We change d with random values of $\theta \sim \mathcal{U}(\pi/4, 3\pi/4)$ and evenly distribute a scatterer with a radar cross-section of 10 m^2 in the plane (this corresponds to a large scattering object) and the forgetting factor β in Algorithm 1 is set to 0.97 [12].

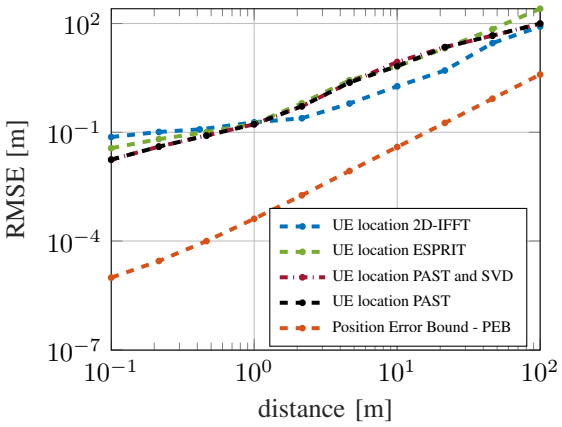

Fig. 2. RMSE curve of the method proposed in this paper PAST, an enhanced variant PAST and SVD, 2D-IFFT [11] and ESPRIT [10] with respect the user distance.

The performance of each estimation method, in terms of position RMSE, as a function of the distance between the UE and the Base Station (BS), is depicted in Figure 2. Besides estimation models, the Position Error Bound (PEB) is also presented in the figure. The PEB represents the minimum error attainable when the position is measured by an unbiased estimator [17]. We observe that the PAST-based estimation exhibits lower position errors than ESPRIT and 2D-IFFT for distances closer to the BS (ranging from 0.1 m to 1 m). This can be attributed to the fact that PAST is an iterative search algorithm that projects data onto a lower-dimensional subspace, refining the DOA estimates with each iteration. However, beyond 1 m of distance, the PAST estimation's RMSE increases compared to the 2D-IFFT DOA estimation. This may occur as the FFT beams approach the far-field beams of each sub-array, which impacts the estimation performance.

The model operates in the near-field regime only when $0.62\sqrt{(N\Delta)^3/\lambda} < ||\mathbf{x}|| < 2(N\Delta)^2/\lambda$ (between 3.4 m and 89 m). Although the 2D-IFFT DOA estimation demonstrates the best performance in terms of RMSE within the near-field distance compared to other methods, its precision is limited. This limitation is evident in Figure 3 and Figure 4, where the CDF curves indicate a higher variance for the estimator compared to the subspace-based methods. We examined estimators' behavior within the near-field region by assessing two distances in this simulation: 3.5 meters (proximal to the antenna) and 25 meters (distant from the antenna), both confined within the near-field range.

The CDF curves of the proposed method exhibit enhanced precision, comparable to that of 2D-IFFT. Additionally, compared to ESPRIT, the curves show a similar performance. However, it is crucial to highlight the lower computational burden of PAST. While the latter has a complexity of $\mathcal{O}(Mr)$

TABLE I
SUMMARY OF THE 10TH, 50TH, AND 90TH PERCENTILES FOR THE CUMULATIVE DISTRIBUTION FUNCTION FOR $||x|| = \{3.5, 25\}m$

	3,5m				25m			
Percentile	**PAST**	**PAST and SVD**	**ESPRIT**	**2D-IFFT**	**PAST**	**PAST and SVD**	**ESPRIT**	**2D-IFFT**
10	0.0250	0.0252	0.0259	0.2090	0.3983	0.2987	0.3847	0.5427
50	0.0251	0.0255	0.0312	0.8065	0.4730	0.3738	0.4103	0.9101
90	0.0253	0.257	0.0373	1.5012	0.5325	0.5025	0.5563	1.3765

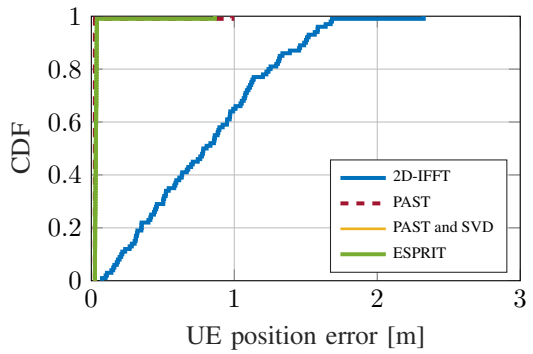

Fig. 3. Comparison of empirical CDFs between estimators, $||x|| = 3, 5$ m.

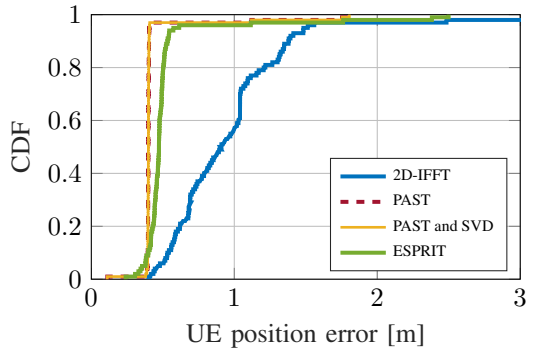

Fig. 4. Comparison of empirical CDFs between estimators, $||x|| = 25$ m.

per sub-array, ESPRIT's complexity is primarily dominated by the SVD, which is $\mathcal{O}(M^3)$. Therefore, the suggested technique shows reasonable needs, making it appropriate for sub-arrays with limited computational restrictions.

We compared the methods using the 10th, 50th, and 90th percentiles. Table I supports the findings in Figure 3 and Figure 4. The 2D-IFFT method has outliers, causing positioning errors over twice that of our method at the 90th percentile. At the 10th and 50th percentiles, all techniques achieve sub-meter accuracy, but our method performs better. Additionally, subspace-based methods have comparable performance.

V. CONCLUSION

In this paper, we have presented a novel localization approach that combines the PAST algorithm and sub-array processing for positioning estimation. We have achieved a balance between low complexity and high-accuracy localization. Our proposed method was compared to other well-known techniques using RMSE and CDF-based statistical analysis. The results show that our approach outperforms these techniques in terms of precision. In future works, we plan to investigate the influence of hardware limitations on individual sub-arrays to bolster the reliability of the subspace estimator.

REFERENCES

[1] B. Friedlander, "Localization of signals in the near-field of an antenna array," *IEEE Transactions on Signal Processing*, vol. 67, no. 15, pp. 3885–3893, 2019. DOI: 10.1109/TSP.2019.2923164.

[2] K. Hu, S. P. Chepuri, and G. Leus, "Near-field source localization using sparse recovery techniques," in *2014 International Conference on Signal Processing and Communications (SPCOM)*, 2014, pp. 1–5. DOI: 10.1109/SPCOM.2014.6983929.

[3] Y.-D. Huang and M. Barkat, "Near-field multiple source localization by passive sensor array," *IEEE Transactions on Antennas and Propagation*, vol. 39, no. 7, pp. 968–975, 1991. DOI: 10.1109/8.86917.

[4] M. Cui, Z. Wu, Y. Lu, X. Wei, and L. Dai, "Near-field communications for 6g: Fundamentals, challenges, potentials, and future directions," *IEEE Communications Magazine*, 2022.

[5] E. Cekli and H. Cirpan, "Unconditional maximum likelihood approach for near-field source localization," in *ICECS 2001. 8th IEEE International Conference on Electronics, Circuits and Systems (Cat. No.01EX483)*, vol. 2, 2001, 753–756 vol.2. DOI: 10.1109/ICECS.2001.957584.

[6] J. Chen, R. Hudson, and K. Yao, "Maximum-likelihood source localization and unknown sensor location estimation for wideband signals in the near-field," *IEEE Transactions on Signal Processing*, vol. 50, no. 8, pp. 1843–1854, 2002. DOI: 10.1109/TSP.2002.800420.

[7] X. Zhou, F. Zhu, Y. Jiang, X. Zhou, W. Tan, and M. Huang, "The simulation analysis of doa estimation based on music algorithm," in *2020 5th International Conference on Mechanical, Control and Computer Engineering (ICMCCE)*, 2020, pp. 1483–1486. DOI: 10.1109/ICMCCE51767.2020.00325.

[8] T. Lavate, V. Kokate, and A. Sapkal, "Performance analysis of music and esprit doa estimation algorithms for adaptive array smart antenna in mobile communication," in *2010 Second International Conference on Computer and Network Technology*, 2010, pp. 308–311. DOI: 10.1109/ICCNT.2010.45.

[9] F.-M. Han and X.-D. Zhang, "An esprit-like algorithm for coherent doa estimation," *IEEE Antennas and Wireless Propagation Letters*, vol. 4, pp. 443–446, 2005. DOI: 10.1109/LAWP.2005.860194.

[10] H. Wymeersch, "A fisher information analysis of joint localization and synchronization in near field," in *2020 IEEE International Conference on Communications Workshops (ICC Workshops)*, 2020, pp. 1–6. DOI: 10.1109/ICCWorkshops49005.2020.9145059.

[11] W. Zhi and M. Y.-W. Chia, "Near-field source localization via symmetric subarrays," *IEEE Signal Processing Letters*, vol. 14, no. 6, pp. 409–412, 2007. DOI: 10.1109/LSP.2006.888390.

[12] B. Yang, "Projection approximation subspace tracking," *IEEE Transactions on Signal processing*, vol. 43, no. 1, pp. 95–107, 1995.

[13] R. Landqvist and A. Mohammed, *The Projection Approximation Subspace Tracking Algorithm Applied to Whitening and Independent Component Analysis in Wireless Communications*. 2005.

[14] Y.-D. Huang and M. Barkat, "Near-field multiple source localization by passive sensor array," *IEEE Transactions on Antennas and Propagation*, vol. 39, no. 7, pp. 968–975, 1991. DOI: 10.1109/8.86917.

[15] S. Rogers, *Adaptive filter theory: By simon haykin. prentice hall; upper saddle river, nj, usa; 1996; 989 pp.;* 84; *ISBN: 0-13-322760-x*, 1996.

[16] J. L. Boldrini, S. I. Costa, V. Figueredo, and H. G. Wetzler, *Álgebra linear*. Harper & Row, 1980.

[17] D. B. Jourdan, D. Dardari, and M. Z. Win, "Position error bound and localization accuracy outage in dense cluttered environments," in *2006 IEEE International Conference on Ultra-Wideband*, 2006, pp. 519–524. DOI: 10.1109/ICU.2006.281603.